

A quantitative assessment of heart phantom motion and its effect on myocardial perfusion SPECT images

SHI Hong-Cheng, CHEN Shao-Liang, Zhang Xin¹, YAO Zhi-Feng,
LIU Wen-Guan, ZHU Wei-Min

(Zhongshan Hospital, Fudan University, Shanghai 200032;

¹Shanghai I & C Foreign Language School, Shanghai 200231)

Abstract In order to study the image characteristics of motion artifacts and to determine the relations of motion artifacts with varied motion types, and the imaging timings, frames, distances and directions during SPECT acquisition, a myocardial phantom filled with pertechnetate solution was used to simulate the patient motion. In nonreturning pattern, the simulation motion was timed at the 0°, -45° and -90° positions during the rotation of the detector over a 180° arc from +45° right anterior oblique to -135° left posterior oblique. Simulation motion was performed by moving the phantom ± 5 mm, ± 10 mm and ± 20 mm along *X*- (from left to right), *Y*- (from head to caudal) and *Z*-axis (from back to ventral) respectively. In returning pattern the acquired 30 projections were divided into three equal parts. The simulation motion was timed at the middle 1-7 projections of each part and performed by moving the phantom ± 5 , ± 10 , ± 15 , ± 20 , ± 25 , ± 30 and ± 50 mm along *X*-, *Y*- and *Z*-axis respectively. Each image was compared with normal image and assessed by three experienced observers without knowledge of the phantom motion. Logistic regression analysis was used to determine the relationship of motion artifacts with the affecting factors. No significant artifacts can be found when the phantom was moved slightly, no matter which motion pattern, direction and timing were taken. The characteristics of motion artifacts showed a radioactive marker dot in inferior wall firstly when the phantom was moved along *X*-axis. Septal and lateral wall became "hot" symmetrically when the phantom was moved along *Y*-axis. And nodular hot could be found in anterior wall when the phantom was moved along *Z*-axis. At last the "lumpy" and "defect" areas existed alternately and formed a triangle respectively. The presence of motion artifacts was related to motion directions, distance and affected frames, but was independent of motion timing. The characteristics of motion artifacts could be found when the phantom was moved along different axis. Motion distance contributed more to the appearance of motion artifacts than other related factors, this was especially clear when motion was along *Y*-axis.

Keywords Heart phantom, Myocardial perfusion SPECT, Motion artifacts

CLC numbers R542.2, R817.4 A

1 INTRODUCTION

Myocardial perfusion SPECT has been widely applied to the diagnosis and evaluation of patients with known or suspected coronary artery disease. Although SPECT was

an accurate, noninvasive diagnostic method for the detection of coronary artery disease, the image artifacts reduce the clinical impact of this technique. It is well known that patient motion during myocardial perfusion SPECT acquisition is very common sources of error in scan interpretation. Many methods have been reported for patient motion correction, but up to now no ideal methods are available. Some authors paid special attention to the findings of motion artifacts. The pattern and severity of motion-induced artifacts have been described for actual or simulated motion varying in type, timing, duration, magnitude, and direction (axis) during SPECT acquisition. All those findings were about typical artifacts lacking a description of the process of the artifacts changing from a slight to typical one. With a view to this situation, heart phantom was used for simulating patient motion to investigate the process of the artifacts changing from slight to typical ones. And the relations between artifacts with motion timing, frames, distance and direction during SPECT acquisition with a single-head detector were studied.

2 MATERIALS AND METHODS

2.1 Image acquisition and processing

A polymethyl methacrylate heart phantom was filled with 0.37 MBq/mL pertechnetate solutions. The direction and position of the phantom was the same with the patient's heart when he was supine on the bed. The SPECT images were acquired on a gamma camera (Apex SP-6, Elscint Company) with a single-head detector using a high-resolution, low-energy collimator, 30 projections over a 180° arc from $+45^\circ$ right anterior oblique to -135° left posterior oblique. The raw projection datasets were filtered with a Butterworth filter: order 5, and cutoff frequency 0.66 cycle/pixel; pixel size, 6.4 mm. No scatter or attenuation correction was applied. Filtered raw projection images were automatically reconstructed into the short-axis, vertical long-axis, and horizontal long-axis images. During acquisition the phantom was moved a certain distance along X (from left to right), Y (from head to caudal) and Z -axis (from back to ventral) respectively. Anytime before the phantom was moved, normal imaging was acquired firstly. Both nonreturning and returning motion pattern were simulated.

Nonreturning pattern: The simulation motion was timed at the 0° , -45° and -90° position during the images acquisitions and performed by moving the phantom ± 5 mm, ± 10 mm and ± 20 mm along X -, Y - and Z -axis respectively. Whenever the phantom was moved, it would not be returned.

Returning pattern: The acquired 30 projections were divided into three equal parts. The simulation motion was timed at the middle 1–7 projections of each part and performed by moving the phantom ± 5 , ± 10 , ± 15 , ± 20 , ± 25 , ± 30 and ± 50 mm along X -, Y - and Z -axis respectively. For instance, in the first part the simulation motion was timed at the 5th, 4th–5th, 4th–6th, 4th–7th, 3rd–7th, 3rd–8th and 2nd–8th projections in turn and performed by moving the phantom a certain distance along different axis respectively as mentioned above. After those projections were acquired, the phantom was returned (Table 1).

Table 1 Motion timing of 1-7 frames in each part in returning pattern*

Timing	Part 1	Part 2	Part 3
	Frame 1-10	Frame 10-20	Frame 20-30
1 frame	5th	15th	25th
2 frames	4th-5th	14th-15th	24th-25th
3 frames	4th-6th	14th-16th	24th-26th
4 frames	4th-7th	14th-17th	24th-27th
5 frames	3rd-7th	13th-17th	23rd-27th
6 frames	3rd-8th	13th-18th	23rd-28th
7 frames	2nd-8th	12th-18th	22nd-28th

*+45° RAO, -135° LPO

2.2 Images interpretation

The images were reviewed and compared with the normal images on a video monitor by 2 experienced observers without knowledge of the phantom moved or not, a third observer reviewed when no consensus was reached. Any "hot" and or "defect" areas appeared on the wall were considered abnormal.

2.3 Statistical analysis

In the nonreturning pattern chi-square tests were used to compare differences between normal and moved group. $p < 0.05$ was considered statistically significant. In the returning pattern Logistic regression analysis were used to analyze the relationship among the presence of motion artifacts with the motion type, timing, frames, distance, and direction during SPECT images acquisition.

3 RESULTS

3.1 Results of the phantom motion

When motion frames and or distances were few, no artifacts were identified visually in nonreturning and returning pattern. In nonreturning pattern when the phantom was moved no more than 5 mm, no matter which timing or direction motion was, no obvious motion artifacts can be identified. When the phantom was moved not less than 10 mm, obvious motion artifacts could be found.

In returning pattern: The image failed to produce significant perfusion defects when the phantom was moved slightly along any axis. With the distance increased, the artifacts appeared gradually and the position of induced defects varied with motion timing and direction (Table 2). For example, when a single frame was moved 50 mm along X- or Z-axis, no obvious artifacts could be found, but artifacts were shown clearly when 1 frame was moved 30 mm along Y-axis at any part. At the same time, the minimal distance caused artifacts decreased with increasing the number of the motion frames. When the motion frames were the same, the minimal distance caused artifacts varied with motion timing and direction. For instance, when 3 frames were involved along X-axis, the minimal distance in part 1, 2, 3 was 15, 10, 20 mm respectively.

Table 2 The appearance of artifacts varied with motion distance and timing

Numbers of motion frame	X-axis (part 1,2,3) (mm)	Y-axis (part 1,2,3) (mm)	Z-axis (part 1,2,3) (mm)
1	No artifacts when moved 50	30,30,30	No artifacts when moved 50
2	50, 20, 50	10, 20, 20	25, 50, 50
3	15, 10, 20	10, 10, 10	10, 10, 10
4	50, 50, 10	50, 50, 50	10, 50, 50
5	50, 50, 50	50, 50, 50	50, 50, 50
6	50, 50, 50	50, 50, 50	50, 50, 50
7	50, 50, 50	50, 50, 50	50, 50, 50

3.2 Artifacts characteristics

In nonreturning pattern: When the phantom was moved 10 or 20 mm, motion artifacts could be identified visually ($p < 0.05$). The artifacts were mainly shown in the short axis slices, the “lumpy” and “defect” areas existed alternately and formed a triangle respectively (Fig.1). In the vertical long axis slices the perfusion defect located in the anterior wall near to the apex. The “lumpy” and “defect” areas became opposite in position when the phantom was moved at the same distance but reverse direction (Fig.2). With the motion distance increased, the “lumpy” and “defect” became more obvious.



Fig.1 The image not moved (A) compared with moved 10mm(B) in nonreturning pattern

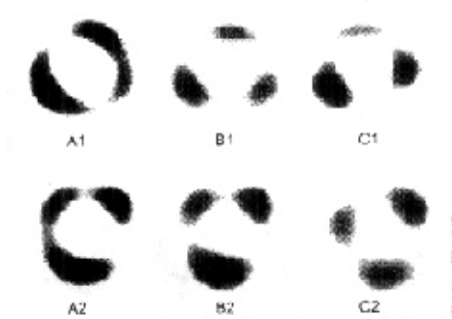


Fig.2 The phantom was moved up and down 20 mm along Z-axis (upper and lower row) timing at 45°(A), 90°(B) and 135°(C)

In returning pattern: Firstly the characteristics of the mild motion artifacts only appeared in short axis slices. The image showed a radioactive marker dot in inferior wall, “hot” area in septal and lateral wall symmetrically and nodular hot in anterior wall when the phantom was moved along X-, Y- and Z-axis respectively (Figs. 3, 4, 5). With motion frames and or distance increased, the hot area became larger and exceeded the outline of the heart phantom wall. In general, the defect size grew with incremental motion frames and or motion distance (Fig. 5, 6). When the motion distance and frames were held constant, defects position and extent depended on the motion timing (Fig.7). At last the typical performance of motion artifacts was gradually similar to that in the

nonreturning pattern.



Fig.3 The phantom was moved right 15 and 20 mm along *X*-axis compared with normal



Fig.4 The phantom was moved head 10 and 15 mm along *Y*-axis compared with normal



Fig.5 The phantom was moved up 25 and 50 mm affected 1 frame along *Z*-axis compared with normal

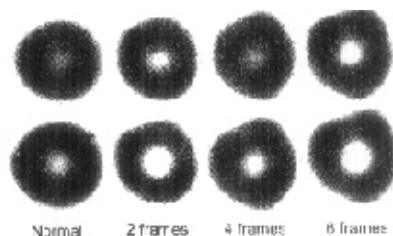


Fig.6 The phantom was moved left 15 mm affected 2, 4 and 6 frames along *X*-axis compared with normal

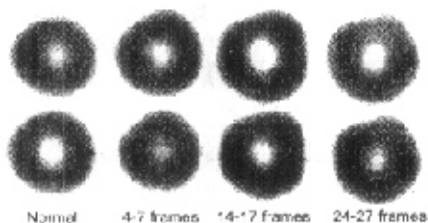


Fig.7 The phantom was moved up 15 mm affected 4 frames and timing at 1, 2 and 3 part respectively along *Z*-axis compared with the normal

3.3 Analysis of factors influencing motion artifacts

Simple regression analysis showed that the presence of motion artifacts was related to motion distance along *Y*-axis, motion frames. The relevance was 0.552 (95% confidence interval was: 0.431-0.707), 0.197 (95% confidence interval was: 0.142-0.273) respectively. But the presence of motion artifacts was independent of timing, motion distance along *X*- and *Z*-axis.

Logistic regression analysis showed that motion artifact was related to motion frames, motion distance along *X*-, *Y*- and *Z*- axis, but was independent of the motion timing. Even regression analysis of every timing in any part was made, no relations between artifacts and motion timing could be found (Table 3).

Table 3 The results of the logistic regression analysis

Variant	Parameter estimate	Standard error	χ^2 value	$p^{(1)}$ value	Standard estimate	OR value (95% confidence interval)
Intercept	10.1999	1.4176	51.7696	0.0001		
Frames	0.0380	0.0275	1.9067	0.1673	0.1724	1.039(0.984,1.096)
Distance	-2.8413	0.3647	60.7061	0.0001	-2.9506	0.058(0.029,0.119)
X axis	-2.5676	0.4207	37.2539	0.0001	-1.9430	0.077(0.034,0.175)
Y axis	-1.3774	0.2636	27.3001	0.0001	-0.9902	0.252(0.150,0.423)
Z axis	-1.7457	0.2890	34.3212	0.0001	-1.1740	0.175(0.097,0.313)

⁽¹⁾ $p < 0.05$ was considered statistically significant

According to the value of the standard regression coefficient, those factors contributed to the motion artifacts in proper order were motion frames, motion distance along Y-, Z- and X-axis. The presence of motion artifacts was independent of the motion timing.

4 DISCUSSION

Although myocardial perfusion imaging with SPECT is an accurate and reliable diagnostic study, artifacts must be avoided, or detected and corrected, thereby to minimize the false-positive rate. Myocardial perfusion SPECT imaging may present a greater frequency of motion artifacts than any other SPECT imaging due to long duration using ²⁰¹Tl and ^{99m}Tc sestamibi intolerable especially in elderly and seriously ill patients. A review of 165 serials clinical SPECT perfusion scintigrams revealed evident motion in approximately 25% of cases. And 5% produced significant artifact.^[1] The best solution to patient motion is to prevent it during SPECT acquisition by, for example, using arm-holding devices or positioning the patient prone for imaging. But all those efforts can only reduce the motion frequency, cannot prevent it happen. Although several motion-correction programs are available to automatically or semiautomatically detect and compensate for motion in the projection datasets, none of these methods have proven robust or sufficiently practical to achieve wide clinical use now. Also motion artifacts can be reduced after acquisition by manual shifting of individual projection images before reconstruction. And sometimes the result was better than corrected by computer software, although this process is time-consuming and subject to operator variability.^[2] So identification of motion artifacts is significant in clinical practice.

Some authors paid special attention to the findings of motion artifacts in clinical work or simulated the patient motion to find the characteristics of motion artifacts.^[1,3,4] For the presence of motion artifacts, only the typical findings were reported. DePuey *et al*^[4] noted the curvilinear tail of activity that extend from the defects, which are characteristics of a motion artifacts on SPECT. This may be the case when the motion was very serious. By simulating the patient motion, Botvinick and his coworkers^[1] found that typical findings included an irregular or lumpy distribution of radioactivity with often opposing defects between the lumpy. Our study results agreed generally with observations of those authors and carried them further. We also found that the image

showed a radioactive marker dot in inferior wall, "hot" area in septal and lateral wall symmetrically and nodular hot in anterior wall when the phantom was moved along X-, Y- and Z-axis respectively. Those findings were very useful for image interpreters to diagnose, as most of the mild motion artifacts were the main sources of misdiagnosis in clinical practice. And patient motion happened mainly in this way. When motion frames and or distances increased, the typical findings mentioned above would appear. The process of motion artifacts changing from slightly to typically had never been reported before our study. At the same time our results told that the "lumpy" and "defect" areas become opposite in position when the motion distance was at the same distance but reverse direction. When motion distance and frames were held constant, defects position and extent varied with the motion timing.

DePuey *et al*^[4] described only the "typical" findings but they did not show what type and degree of patient motion would routinely cause scan artifacts. Eisner *et al*^[5] suggested that patient motion as little as 1 cm could cause a significant image artifact. While this may be the case when many frames were affected, the situation was clearly more complex. Other authors^[1,6] described the situation detailed by simulating the patient motion. They found that slight motion failed to produce significant perfusion defects. Motion artifacts were related to the motion frames, distance and directions. By simulating the patient motion with computer Botvinick *et al*^[1] found that 8 pixel upward motion affecting 2 frames would cause artifacts. Displacement of 3 pixels produced an image artifact when affecting 4 frames. Matsumoto and his fellows^[6] reported that 3 frames shifting 1-pixel did not create a significant perfusion defect, but when shifting three-pixel usually produced severe perfusion defects. Our study showed that when only 1 frame moved along X-axis or Y-axis, even moved 50 mm, no artifacts could be found; when 3 frames moved 15, 10, 20 mm along X-axis would cause visual artifacts in part 1, 2, 3 respectively. The minimal distances causing artifacts were different among the investigators because the sensitivity of the SPECT machine, the experience of the interpreter and the style of the simulation motion were different. Now a heart phantom was used for the first time to simulate patient motion in three-dimensional way and the results were more close to the clinical patient motion than those two-dimensional simulation of patient motion.

The pattern of the patient motion during SPECT acquisition was unexpected. Some literatures^[7,8] supported returning motion would appear uncommon during SPECT acquisition. Eisner *et al*^[5] noted that multiple episodes of patients' motion were the "more general case." In any motion pattern, the image failed to produce significant perfusion defects when the motion was mild, and the typical findings were the same when the motion was serious.

The presence and extent of motion artifacts varied with the frames and timing of the affected projection image, as well as the distance and direction of their displacement. Which factor would have great effect on artifacts had never been reported. By means of Logistic regression analysis and according to the value of the standard regression coefficient, we found that those factors contributing to the motion artifacts in proper

order were motion frames, motion distance along *Y*-, *Z*- and *X*-axis. This result indicates the image interpreter and technologist that what should be done first to avoid motion artifacts during image data acquisition if possible.

In clinical practice, patient motion during topography can be detected by inspection of the dynamic display of the projection images. Inspection of the image sinogram may also be helpful. But all those information can be got only in the computer's screen and was always ignored by the technologist and interpreter. It is obviously important to recognize the presence of motion artifacts and the observations here help to relate this observation to SPECT findings in clinical.

5 CONCLUSION

The current study analyzed the pattern and extent of perfusion defects produced by using heart phantom simulating patient motion during image acquisitions with a single-head detector. Mild motion failed to produce artifacts. The presence of a radioactive marker dot in inferior wall, "hot" area in septal and lateral wall symmetrically, nodular hot in anterior wall were shown when the phantom was moved a certain distance along *X*-, *Y*- and *Z*-axis respectively. The typical findings could be found mainly in the short axis slices. Furthermore the artifacts showed the "lumpy" and "defect" area existed alternately and formed a triangle respectively. By means of Logistic regression analysis and according to the value of the standard regression coefficient, motion frame was the most important factor contributing to the presence of motion artifacts among the related factors.

References

- 1 Botvinick E H, Zhu Y Y, O'Connell W J *et al.* J Nucl Med, 1993, **34**(2):303-310
- 2 O'Connor M K, Kanal K M, Gebhard M W *et al.* J Nucl Med, 1998, **39**(10):2027-2034
- 3 Shi H C, Li W G, Chen S L *et al.* Chin J Nucl Med, 2000, **20**(3):109-111
- 4 DePuey E G, Garcia E V. J Nucl Med, 1989, **30**(4):441-449
- 5 Eisner R L, Noever T, Nowak D *et al.* J Nucl Med, 1987, **28**(1):97-101
- 6 Matsumoto N, Berman D S, Kavanagh P B *et al.* J Nucl Med, 2001, **42**(5):687-694
- 7 Eisner R, Churchwell A, Nover T *et al.* J Nucl Med, 1988, **29**(1):91-97
- 8 Friedman J, Train K V, Maddahi J *et al.* J Nucl Med, 1989, **30**(10):1718-1722